# Large soil carbon storage in terrestrial ecosystems of Canada

Camile Sothe[1], Alemu Gonsamo[1], Joyce Arabian[2], Werner A Kurz[3], Sarah A Finkelstein[4], and James Snider[2]

[1]McMaster University
[2]WWF-Canada
[3]Natural Resources Canada
[4]University of Toronto

November 30, 2022

## Abstract

Terrestrial ecosystems of Canada store a large amount of organic carbon (C) in soils, peats and plant materials, yet little is known about the C stock size and distributions, both spatially and in various C pools. As temperature rises, C is becoming available for disturbance, decomposition and eventual release into the atmosphere, which makes the quantification of C stocks in terrestrial ecosystems of Canada of high interest for the assessment of climate change impacts and conservation efforts. Here, we use multisource satellite, climate and topographic data and a machine-learning algorithm to produce the first wall-to-wall estimate of C stocks in plants and soils of Canada at 250 m spatial resolution. Our findings show that above and belowground live biomass and detritus store a total of 21.1 Pg C. Whereas the Canadian soils store 313 Pg organic C in the top 1 m, 83 Pg C of which are stored in peatlands, confirming that soil organic C dominates terrestrial carbon stocks. We also find previously under-reported large soil organic C stock in forested peatlands on the boreal shields of Canada. Given that Canada is warming twice the global average rate and Canadian soils store approximately 20% of world soil C stocks in top 1 m, initiatives to understand their vulnerabilities to climate change and disturbance are indispensable not only for Canada but also for the global C budget and cycle.

## Hosted file

`sothe_et_al_agusupporting-information.docx` available at https://authorea.com/users/559896/articles/608217-large-soil-carbon-storage-in-terrestrial-ecosystems-of-canada

# Large soil carbon storage in terrestrial ecosystems of Canada

**C. Sothe,[1]* A. Gonsamo,[1] J. Arabian,[2] W. A. Kurz,[3] S. A. Finkelstein,[4] J. Snider[2]**

[1]School of Earth, Environment & Society, McMaster University, Hamilton, Ontario, Canada.

[2]World Wildlife Fund Canada, Toronto, Ontario, Canada.

[3]Canadian Forest Service, Natural Resources Canada, Victoria, British Columbia, Canada.

[4]Department of Earth Sciences, University of Toronto, Toronto, Ontario, Canada.

Corresponding author: Camile Sothe (sothec@mcmaster.ca)

**Key Points:**

- Our findings indicate Canada's soils store 313 Pg organic carbon in the top 1 m, which is 20% of the global soil carbon storage.
- Peatlands, covering ~12% of Canada, store 26.5% of the total amount of the soil organic carbon storage of the nation.
- We find previously unreported large organic carbon stock in forested boreal peatlands of Canada.

## Abstract

Terrestrial ecosystems of Canada store a large amount of organic carbon (C) in soils, peats and plant materials, yet little is known about the C stock size and distributions, both spatially and in various C pools. As temperature rises, C is becoming available for disturbance, decomposition and eventual release into the atmosphere, which makes the quantification of C stocks in terrestrial ecosystems of Canada of high interest for the assessment of climate change impacts and conservation efforts. Here, we use multisource satellite, climate and topographic data and a machine-learning algorithm to produce the first wall-to-wall estimate of C stocks in plants and soils of Canada at 250 m spatial resolution. Our findings show that above and belowground live biomass and detritus store a total of 21.1 Pg C. Whereas the Canadian soils store 313 Pg organic C in the top 1 m, 83 Pg C of which are stored in peatlands, confirming that soil organic C dominates terrestrial carbon stocks. We also find previously under-reported large soil organic C stock in forested peatlands on the boreal shields of Canada. Given that Canada is warming twice the global average rate and Canadian soils store approximately 20% of world soil C stocks in top 1 m, initiatives to understand their vulnerabilities to climate change and disturbance are indispensable not only for Canada but also for the global C budget and cycle.


**Keywords:** Carbon stock mapping; Peatlands; Soil; Satellite data; Machine learning.

## 1 Introduction

Terrestrial ecosystems store large quantities of carbon (C) in plants and soils, playing an important role in determining the state of the global climate system undergoing rapid human-induced changes (Heimann and Reichstein, 2008; Xu et al., 2018; Harris et al., 2021). Temperatures are increasing faster at mid- to high latitudes and over the continental landmasses as Canada (Bush and Flato, 2019), where terrestrial ecosystems net primary productivity (NPP) is estimated as 1.27 petagram of carbon (Pg C) annually, of which forests alone contribute 1.02 Pg C (Gonsamo et al., 2013). With increasing scientific and political interest in regional aspects of the global C cycle, there is a strong impetus to better understand the net C storage of terrestrial ecosystems of Canada, which comprise about 9% of world's forests and more than one third of the world's peatlands, characterized by areas with large soil organic carbon (SOC) stock (Minasny et al., 2019).

Plants store about 80% of the live biomass on Earth, with an estimated pool of 450 Pg C (Bar-On et al., 2018). Of those, approximately 70% is stored in aboveground biomass (AGB) of forest areas, with estimates varying from about 290 Pg C (FAO et al., 2020a, Spawn et al., 2020) to 320 Pg C (Bar-On et al., 2018). AGB includes all vegetation above the ground (i.e. stems, branches, barks, seeds, flowers, and foliage of live plants) and is one of the most visible and dynamic terrestrial ecosystem C reservoirs (Kumar and Mutanga, 2017). It differs from SOC pools which are not as readily oxidized (Davidson and Janssens, 2006) as AGB is in a continuous state of flux due to impacts such as fire, logging, storms, land-use changes, and thus their contribution to atmospheric C fluxes is more immediate. In fact, projected increases in the frequency, extent and severity of high-latitude disturbance in North America boreal forests may limit the potential of these ecosystems to serve as a terrestrial C sink (Wang et al., 2021). Estimating C stock is therefore a critical step to monitor C dynamic responses and vulnerabilities to global change.

The existing national inventory estimates only report C stock in AGB and belowground biomass (BGB) in managed forests of Canada, which comprise 65% of the country's forests (FAO et al., 2020b). AGB estimates at national level were also provided by Beaudoin et al. (2014) who correlated National Forest Inventory (NFI) data with satellite reflectance data and climatic and topographic variables to quantify and produce AGB maps for 12 Canadian ecozones. Later, Matasci et al. (2018a) correlated AGB samples estimated from airborne light detection and ranging (LiDAR) with satellite reflectance and topographic data to map and quantify AGB in 8 Canadian ecozones located in the boreal forest area. Matasci et al. (2018b) included Landsat historical data and expanded predictions to transition between boreal and temperate forest areas. Through such AGB mapping approaches, it is possible to estimate the C stock in live plants, but there is still a lack of information regarding the spatial distribution of C stock in BGB, dead plants, and vegetation of non-forest areas. Besides that, although these studies used LiDAR as a way to increase the number of field samples, none of them used such data to extract and include forest structural variables as AGB predictors, which is imperative considering that optical data can saturate at low AGB levels (Rodríguez-Veiga et al., 2017). LiDAR data usually show the highest correlation with AGB due to their ability to penetrate the forest canopy and detect the forest vertical structure (Goetz and Dubayah, 2011). The use of LiDAR to map biomass was first limited to terrestrial or airborne platforms at plot and local scales but has been recently expanded to continental and global scales with the launch of LiDAR sensors onboard satellites, such as the Ice, Clouds, and Land Elevation Satellite (ICESat) and, more recently, ICESat-2 and Global Ecosystem Dynamics Investigation (GEDI) missions (Narine et al., 2019; Qi et al., 2019; Duncanson et al., 2020). In this sense, the inclusion of canopy structural information derived from LiDAR, could provide improved estimates of C stock in Canadian forests.

Global soils store more C than vegetation and the atmospheric reservoirs combined, with an average of 1,500 Pg C in the top meter alone (Scharlemann et al., 2014), although with considerable spatial variability. Peat soils comprise about one-third of the global SOC stock estimated for the first meter (Scharlemann et al., 2014). Canada, with an estimated 1.1 million km² of peatlands (Tarnocai et al., 2011), likely has the second largest SOC stock of the world (FAO, 2018). Soils that hold larger C stocks such as Canadian peatlands can significantly impact global climate via positive and negative feedbacks associated with changes in C dynamics (Packalen et al., 2014). Paleoecological studies suggest that northern peat soils have been a net C sink, cooling the climate over the Holocene (Gallego-Sala et al., 2018) but may become a C source in this century due to climate warming and drying, coupled with permafrost thaw (McLaughlin et al., 2018; Hugelius et al., 2020; Loisel et al., 2021). As temperature rises, the anaerobic decomposition of perennially frozen peatlands can be accelerated, producing $CH_4$ (Tarnocai, 2009), a gas that is 25 times more effective as a greenhouse gas than $CO_2$ (IPCC, 2007). With warming temperature, aerobic decomposition is expected to increase in unfrozen peatlands (Christensen, 1991) and peat fires are increasing due to peat drying (Thompson et al., 2019), both leading to increased release of peat SOC that has been accumulating for millennia (Hengeveld, 2000; Turetsky, 2015; Loisel et al., 2021).

Global SOC maps, such as SoilGrid initiatives (Hengl et al., 2014; 2017), GSOCmap (FAO, 2018), Harmonized World Soil Database (HWSD and HWSDa) (FAO et al., 2012; Köchy et al., 2015; Batjes et al., 2016) were built without an adequate amount of ground measurements in Canadian peatlands and only report SOC stock for the first 30 cm or top 1 m, which is insufficient to account the potential C stored in northern peatlands that has an estimated average depth of approximately 2.5 m (Hugelius et al., 2020). Previous studies suggest that peatlands in Canada contain approximately 147 Pg C (Tarnocai, 2006), and the Hudson Bay lowland, one of the largest peatland complexes in the world (Yu, 2012), has an average of 100 kg $m^{-2}$ of permafrost C (Hugelius et al., 2014) and stores 30 Pg C (Packalen et al., 2014, Gonsamo et al., 2017). Despite the large storage of C in Canadian terrestrial ecosystems, the country still lacks spatially detailed information of C stocks in various pools, particularly in deep soils that properly represent peatlands. While recent progress has been made (Webster et al., 2018; Minasny et al., 2018; Mahdianpari et al., 2020), high resolution maps of Canadian peatlands remain incomplete, particularly in “unmanaged” regions. The spatial distribution of C stocks in Canadian peatlands is also incompletely mapped with insufficient field data from many regions and from some peatland types including forested peatlands (Bona et al., 2020). Peat depth is a critical variable in the stock estimates and is an important data gap (Hugelius et al., 2020). Thus, improved estimates of the size and spatial distribution of C stocks at the national level for Canada are urgently needed. Such estimates allow for the incorporation of landscape-specific features, reducing the uncertainties produced in global-scale estimates.

Here, for the first time, wall-to-wall estimates of C stock in various pools of terrestrial ecosystems of Canada are provided in one single study. The C stocks are estimated for plants and soil, including AGB of forest, BGB of forest, non-treed vegetation, dead plant materials, and SOC stock in the top 1- and 2-meter depths for entire Canada. For this, we used ground data records and a rich database mainly composed of long-term satellite data, topographic and climate variables associated with a machine learning algorithm, providing C stock maps at 250 m spatial resolution. The uncertainties related to C stock estimates in soil and AGB were also provided in this study.

## 2 Materials and Methods

### 2.1 Reference forest inventory data

Samples for the C stock of plants in forested areas were compiled from the AGB measurements from four Canadian provinces (Fig. S1a). The AGB samples in Mg $ha^{-1}$ from New Brunswick, Quebec and Saskatchewan were acquired from the NFI (nfi.nfis.org) archive, totaling 216 plots with AGB and dead plant materials information, collected in 2006. For British Columbia, samples were acquired from provincial data (catalogue.data.gov.bc.ca), which contains a large dataset of forest attributes, including AGB, collected for many years. We selected 47,751 forest plots corresponding to the years 2015 to 2019 in order to match with the date of most remote sensing data.

### 2.2 Reference soil carbon content data

The soil ground measurements were acquired from the World Soil Information Service (WoSIS) (https://www.isric.org/) (Fig. S1b). This service provides a standardized compilation of soil data of the entire world (Ribeiro et al., 2015; Batjes et al., 2017). In Canada, the WoSIS database contains SOC data (in g C $kg^{-1}$) in 6,490 locations for 39,323 soil vertical profiles. The soil samples account for organic matter (i.e. O and LFH horizons) (Pennock et al., 2015). Additional samples from peatlands were acquired from the Lehigh University Peatlands Database (Loisel et al., 2014) for 43 sites and 298 soil profiles.

## 2.3 Explanatory environmental data

We selected 78 covariates to model forest AGB, such as spectral bands in the red, red-edge, near infrared (NIR) and short-wave infrared (SWIR) regions, seasonal spectral indices computed from Landsat-8, Sentinel-2 or MODIS data, terrain parameters such as digital elevation model (DEM), slope and topographic indices, structural parameters (e.g., Synthetic Aperture Radar (SAR) data, clumping index, canopy height percentiles, the latter generated from satellite LiDAR observations), soil type map and radiation flux data, the latter to account the latitudinal gradient of the country (Table S1). Most of these covariates were averaged over 5 years (2015 to 2019) of data collection depending on data availability.

In order to incorporate canopy height information into the AGB model, we created wall-to-wall height metrics (maximum height, heights at 85th and 95th percentiles) using ATL08 LiDAR products (Neuenschwander and Pitts, 2019) from ICESat-2 satellite. The data were download for one-year period (October 2018 to October 2019). After filtering solar background noise and atmospheric scattering, 49,959 points distributed over all of Canada were associated with 10 ancillary variables. primarily corresponding to structural information derived from Sentinel-1, ALOS-2/PALSAR-2 and clumping index. Afterwards, a random forest (RF) algorithm was used for spatially continuous prediction of height information for all of Canada (Fig. S2).

Forty covariates were included as SOC forming factors, such as long-term average annual precipitation, average annual and bimonthly temperature, spectral bands of Landsat-8, SAR data, annual and seasonal vegetation indices from Landsat-8 and MODIS, terrain parameters, soil type map and soil depth (Table S2). Most of these variables represent the average of 20 years of data collection (2000 to 2019 according to the data availability) to provide a better indication of soil characteristics by portraying the cumulative influence of living organisms on soil formation (Hengl et al., 2017).

Finally, all SOC and forest AGB covariates were resampled (downscaled or upscaled) to 250m spatial resolution in preparation for C stock mapping.

## 2.4 Plant carbon stock estimation

First, we predicted the AGB of forest areas, in which the AGB ground measurements (predictor variable) were overlaid with the AGB covariates (response variables) to compose the regression matrix. Different models were trained using a recursive feature elimination, random forest (RFE-RF) (Breiman, 2001) scheme and a 5-fold cross-validation assessment. The model with higher $R^2$ and lowest root mean square error (RMSE) was used for spatial prediction of AGB in forest areas.

After generating the forest AGB map, the root biomass (or BGB) of forest areas was estimated using relationships between AGB and BGB developed per plant functional type (i.e. deciduous, needleleaf and mixed forest) from ground measurements (Li et al., 2003). The dead plant materials of forest areas were computed by a linear relationship developed between dead plants and AGB from the NFI data archive. The AGB in non-forest areas was estimated using the relationship between non-forest AGB and normalized difference vegetation index (NDVI) of Landsat-8 satellite provided by Zhang et al. (2020). Considering that 50% of biomass is composed of C (IPCC, 2006), we multiplied the biomass of forest and non-forest areas, as well as dead plant materials and root biomass by 0.5 to provide the total C stock in Pg, and maps in kg C $m^{-2}$.

## 2.5 Soil organic carbon (SOC) stock estimation

For SOC estimation, the soil ground measurements (predictor variable) containing x and y coordinates, and depth, were overlaid with the SOC covariates (response variables). Following the approach proposed by Hengl and MacMillan (2019), depth values were specified as the mid-points of horizons thinner than 15 cm. For thicker horizons, upper- and lower-bound depths were assigned, i.e. the values of target variables are copied twice so that the model recognizes at which depths values of properties change, allowing for 3D modelling. Using this method and including the depth as a covariate, a single model could be used to predict SOC at any arbitrary depth, reducing the need for making complex assumptions about the downcore trends in SOC, and maximizing the use of collected data (Sanderman et al., 2018).

Using a similar approach as was done for AGB estimates, different models were trained for SOC estimation using an RFE-RF scheme and a 5-fold cross-validation assessment. The best model was used for spatial prediction of SOC over Canada at intermediate depths between 0 and 2m. Afterwards, the SOC content map of each horizon was converted to SOC stock (kg C $m^{-2}$) using the approach provided by Nelson and Sommers (1982). For this, it was necessary to include coarse fragment information, acquired from the Canadian National Soil Database (NSDB, 2011), and bulk density (BD), estimated using a pedo-transfer function that addresses both organic and mineral soils (Hossain et al., 2015) (Equation 1). The function was chosen because it showed the highest correlation with the SOC content of the ground measurements.

$$BD(g\ cm^{-3}) = 0.71 + 1.322\exp(-0.071 \times SOC\%) \quad (1)$$

The horizons were added to complete each of the two depth intervals used (i.e., 0-1m, 0-2m), and each one was multiplied by the root depth fraction (NSDB, 2011) to discount shallow soils. We removed ice/snow and water areas based on the Land Cover of Canada Map (Government of Canada, 2019) because these do not accumulate soils. Finally, SOC stock estimates were multiplied by the 250×250m grid area to provide the total SOC in Pg C. We also computed the total SOC stock of peat soils in Canada defined as areas with more than 30% probability of peat occurrence (Tarnocai et al., 2011; Xu et al., 2018), resulting in ~1.13 million $km^2$ of peatlands, which is similar to other national estimates (Minasny et al., 2019).

## 2.6 Uncertainty estimation

To build the uncertainty maps, we used the quantile regression forest proposed by Meinshausen (2006). This method can quantify the confidence or certainty in the prediction using prediction intervals. A prediction interval is an estimate of an interval into which the future observations will fall with a given probability. For instance, instead of recording the mean value of response variables in each tree leaf in the forest, the quantile regression records all observed responses in the leaf. The prediction can then return not just the mean of the response variables, but the full conditional distribution of response values for every pixel (Meinshausen, 2006). Using the distribution, it is possible to create prediction intervals for new instances by using the proper percentiles of the distribution.

In this study, we computed the upper (Q90) and lower (Q10) percentiles of SOC and AGB predictions for each pixel. The uncertainty was estimated as the difference between the 90th (Q90) and the 10th (Q10) percentiles SOC and AGB predictions.

## 3 Results

### 3.1 Carbon stock estimation accuracy

Among the 78 explanatory variables, a RF model with 58 covariates reached the best performance for estimating AGB in forest areas, with $R^2$ of 0.52 and RMSE of 52.6 ± 0.4 Mg $ha^{-1}$ (Fig. 1a). The ranking with variables importance (Fig. S3a) showed that the canopy height metrics estimated from satellite LiDAR were the most important features to predict AGB, followed by SAR data from ALOS-2/PALSAR-2, Landsat-8 spectral bands and vegetation indices. For SOC estimation, a RF model with 25 covariates reached the best accuracy, explaining 83% of variability in SOC content across the country (Fig. 1b), with RMSE of 58.6 ± 0.4 g $kg^{-1}$. Depth was the most important covariate for predicting SOC (Fig. S3b), followed by DEM, climate features (long-term mean temperature and precipitation), and finally vegetation indices.

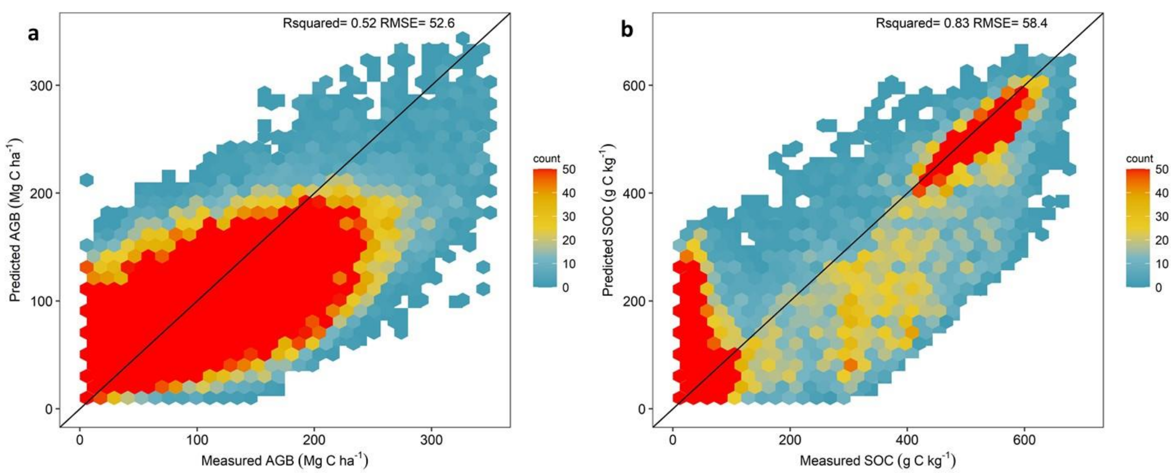


**Figure 1.** Relationship between the measured and estimated carbon (C) stocks using a 5-fold cross-validation assessment and a random forest algorithm. Point density is indicated with a blue (low-density regions) to red (high-density regions) colour gradient. The black line represents a linear fit line. (a) The aboveground biomass (AGB) estimates for forest areas using 58 covariates and 47,967 ground measurements. (b) The soil organic C (SOC) estimation using 25 covariates and 39,621 ground measurements distributed in 0 – 4m soil depth and 6,533 locations.

### 3.2 The size and distribution of organic carbon stocks in terrestrial ecosystems of Canada

Our results indicate that trees in forested ecosystems store a total of 14 Pg C with an average stock of 4.4 kg C $m^{-2}$ in AGB (Fig. 2a, Table 1) and 4.3 Pg C with average of 1.3 kg C $m^{-2}$ in tree roots (Fig. 2b). We also found 2.6 Pg C storage with average of 0.8 kg C $m^{-2}$ in dead plant materials of the forested ecosystems (Fig. 2c). Plants of non-forest areas store a total of 0.2 Pg C with average of 0.04 kg C $m^{-2}$ (Fig. 2d). The total C stock in plants including AGB, plant roots, dead plant materials and non-forest ecosystems was estimated to be 21.1 Pg C for 2015 – 2019 (Fig. 3a). It should be noted that forest disturbances and regrowth that may have occurred during this period are not accounted for and may affect the accuracy of our estimates. In forest ecosystems, the spatial distribution of C stock follows a clear latitudinal gradient, decreasing with increasing latitude (Fig. 3a). Montane and Pacific ecosystems of western Canada characterized by mild climate store the largest plant C on average (>5.5 kg C $m^{-2}$) followed by forests in typical boreal ecosystems (>5 kg C $m^{-2}$) (Fig. S4).

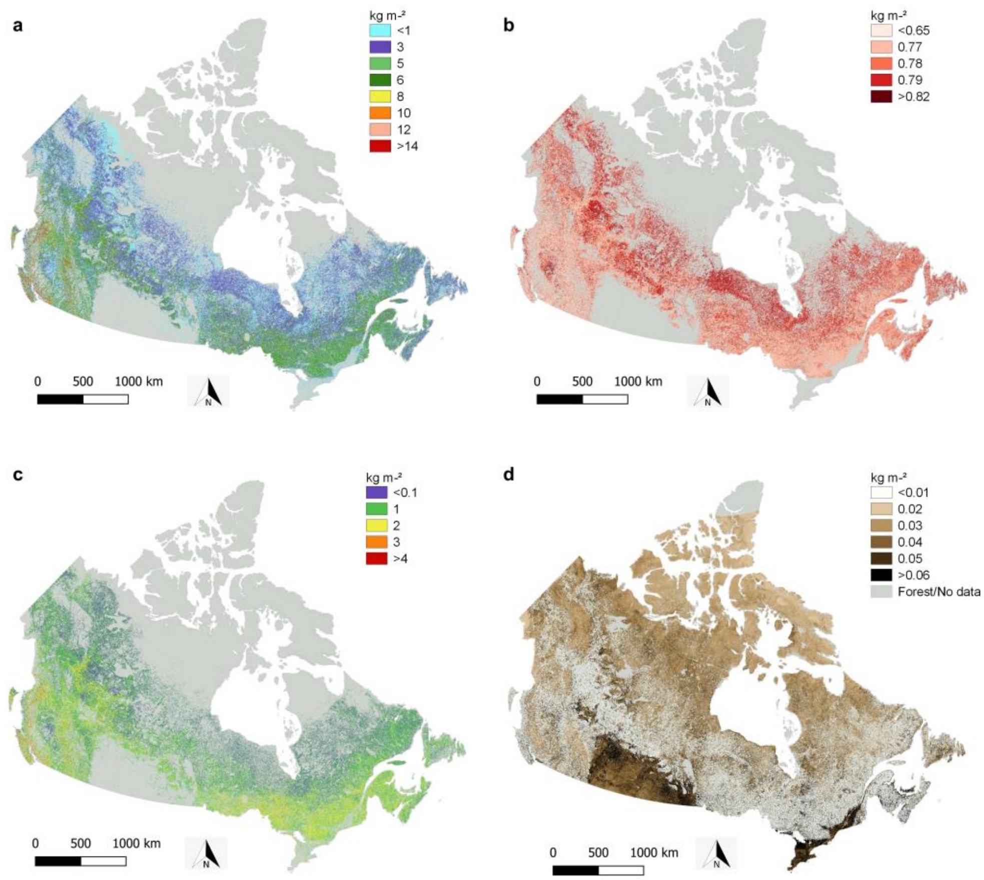


**Figure 2.** C stock distribution in dead and live plant components in kg C $m^{-2}$ at 250 m spatial resolution for years 2015 – 2019. (a) C stock in live plants of forest ecosystems generated by the random forest model and 58 covariates. (b) C stock in plant roots of forest ecosystems generated using relationships between aboveground and root biomass for different forest types (Li et al., 2003). (c) C stock in dead plants of forest ecosystems generated by a linear relationship between aboveground biomass and dead plant materials. (d) C stock in plants of non-forest areas generated using Landsat-8 satellite reflectance observations (Zhang et al., 2020).

The SOC stock estimated in Canada in the top one meter is 313 Pg C (37 kg $m^{-2}$), while additional 203 Pg C is stored between the first- and second-meter depth (Table 1). Canadian peatlands store 83 Pg C and 142 Pg C at depth intervals 0-1 m and 0-2 m, respectively. The Hudson Plain ecozone, with an area of 349,000 $km^2$, alone stores 28 Pg C in the first meter depth (an average of 82 kg $m^{-2}$) and 52 Pg C at 0-2 m depth. Besides the Hudson Plain, our map also shows a previously under-reported SOC pool located in eastern Manitoba (Fig. 3b). That particular region belongs to the Boreal Shield ecozone and reaches an average of 135 kg C $m^{-2}$ in the first meter, even higher than the average observed in the Hudson Plain ecozone, suggesting the need for more field studies of forested peatlands including peat depths and soil C densities in eastern Manitoba.

**Table 1.** Mean (± standard deviation, sd) and total organic C stocks estimated for plant components and two soil depths and peatlands in Canada.

| Organic C stock | Mean ±sd (kg $m^{-2}$) | Total (Pg C) |
|---|---|---|
| AGB (forest) | 4.13±1.80 | 14 |
| Plant roots (forest) | 1.28±0.36 | 4.3 |
| Dead plants (forest) | 0.78±0.02 | 2.6 |
| AGB (non-forest) | 0.04±.01 | 0.2 |
| Soil 0–1 m depth | 37.1±26 | 313 |
| Soil 0–2 m depth | 61.2±47 | 516 |
| Peat soils 0-1 m depth | 63.3±38 | 82.8 |
| Peat soils 0-2 m depth | 109±76 | 142 |

The uncertainty maps (Fig. 3c and 3d) were obtained based on upper and lower quantiles of AGB and SOC prediction, the latter for the top 1 m depth using the quantile regression forest method. It is observed that greater uncertainty is located in regions with higher AGB or SOC values. For soil, those regions correspond to the Hudson Plain and portions of the Boreal Shield and Southern Arctic ecozones while for AGB, the higher uncertainty is located in the Pacific Maritime ecozone.

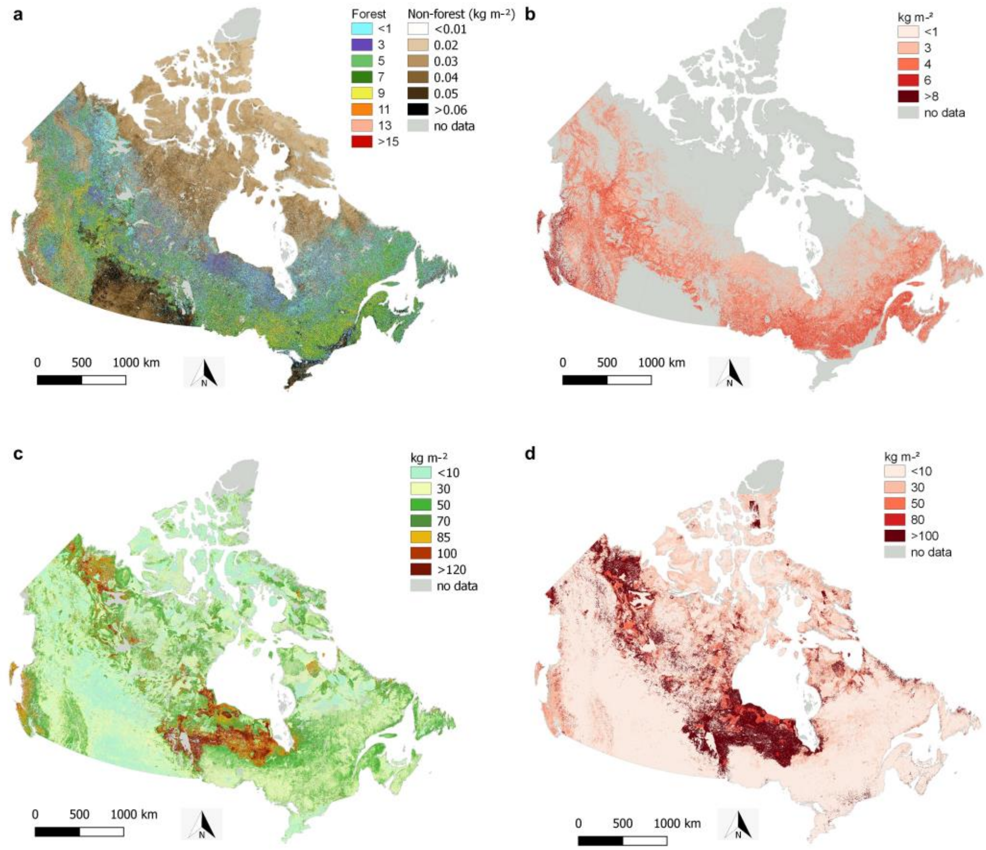


**Figure 3.** The spatial distribution of organic C stocks in kg C m-2 at 250 m spatial resolution. (a) Total C stock of plants in forest and non-forest areas for 2015 – 2019. (b) Total soil organic C stock in 1 m depth. (c) Modelling uncertainty of the plant C stock prediction in forest ecosystems generated with the random forest quantile regression approach. (d) Modelling uncertainty in the soil organic C spatial prediction for 1 m depth generated with the random forest quantile regression approach. Note: water and ice/snow areas were included in the class ‘no data’.

## 4 Discussion

### 4.1 Organic carbon stocks of Canada relative to global estimates

We found that forests store approximately 18.3 Pg C in live plants, including their roots, while plants in non-forested ecosystems store 0.2 Pg C. The former value represents around 6.2% of the total C in forest ecosystems globally according to recent reports of FAO (2020a), highlighting the magnitude of Canada’s forests in the global scale. Canada is among the six largest forested countries that account for 60% of the net flux of Greenhouse Gas (GHG) (Harris et al., 2021) while its forested ecosystems were estimated to be responsible for a net increase of 2.7 Pg C stored in biomass over a 30-year period (Wulder et al., 2020). Previous estimates of C stock in AGB and BGB in forested areas of Canada (Kurz and Apps, 1999) reported 11.5 Pg C and 3 Pg C, respectively, which are lower than the values reported by our study, i.e. 14 in AGB and 4.3 Pg C in BGB. Nevertheless, our findings agree with recent estimates of C stock in AGB compiled from the NFI data that report 14.8 Pg C in 'forest land' of 12 ecozones (NFI, 2016), and 13.6 Pg C and 14.5 Pg C reported for forest areas of 10 and 12 ecozones by Matasci et al. (2018b) and Beaudoin et al. (2014), respectively. The latest estimates of FAO (2020b) suggest 12.7 Pg C is stored in AGB and BGB of managed forest areas in Canada (~2.3 million km²), which is also in line with our study that reports 10 Pg C in AGB and 3 Pg C in BGB when estimates are restricted to managed forests. At a global scale, Spawn et al. (2020) provided spatial estimates of C stock in AGB and BGB. When restricting their estimates to forested areas of Canada, we observed that the C stock values are similar to those reported in this study, approximately 13 Pg C in AGB and 5 Pg C in BGB. Regarding the spatial distribution, the C stock maps of these previous studies (Beaudoin et al., 2014; Matasci et al., 2018b; Spawn et al., 2020) pointed the greatest amount of AGB in the Montane Cordillera and Pacific Maritime ecozones, which agrees with our findings (Fig. 3a and Fig. S4). These ecozones belong to the hemi-boreal zone, a transition between temperate zone and boreal zones and characterized by high canopy height values (approximately 40 m) and large and old trees. Among the forested ecozones, Taiga Cordillera presented the lowest C stock in plants, which was also observed by Matasci et al. (2018b), who reported that the alpine and mountainous conditions of this ecozone are responsible for its low forest cover.

Although Canada has large forest ecosystems that store a significant amount of C, in a global context, Canada stands out even more when it comes to SOC stocks. Canada stores 12% of the global SOC stock in the top 30 cm depth, only behind Russia according to FAO (2018). Nevertheless, FAO (2018) reported a SOC stock of 80.2 Pg C in Canada whereas if we limit our maps to the top 30 cm depth, we report 133 Pg C, very close to the amount that FAO reported for Russia (147 Pg C). Besides different covariates and methods, other explanations for the observed discrepancies include the fact that the FAO estimates are based on less than half the number of samples compared to our study, lack samples in peatlands, and the FAO model is based on global relationship between the explanatory variables and SOC that could bias towards C poor mineral soils, underestimating the SOC stock.

When comparing global SOC maps, Tifafi et al. (2017) showed that the differences in SOC estimation were much greater in the boreal regions and suggested the need for production of country-specific maps to explain this high discrepancy in current global SOC estimates. Indeed, the spatial distribution of SOC stock in some of the existing global maps does not fully corroborate what was observed in our maps (see SoilGrid250m 2.0, https://soilgrids.org/; last access: January 30, 2021). For instance, the SoilGrid250m map indicates that the highest SOC stocks are in the Province of Quebec and in the Pacific Coast region, rather than in the Hudson Plain. Although SoilGrids250m was made using an approach similar to ours, i.e. incorporating soil ground measurements provided by WoSIS and a large number of remote sensing covariates associated with machine learning methods, the model was trained using global data. To address these gaps, we included additional samples from peatlands, trained the model specifically for Canada, and used different covariates to specifically capture soil formation, e.g., those provided by Daymet, Landsat-8 temperature, and a national soil type map (Table S2). In addition, we used bulk density, coarse fragment and root depth information specific for Canada to correct the final SOC stock estimates. This study provides improved SOC stock estimates compared to those made on global scales, such as FAO (2018) and SoilGrid250m (Hengl et al., 2017) because the specificities of Canada were considered. Moreover, our estimates are not restricted to the top 30 cm soil depth.

In fact, we report even larger SOC stocks in deeper soils. Our study indicates 313 Pg C of SOC stock in the top meter, a value almost 4 times higher than the 80.2 Pg C reported by FAO (2018) for the top 30 cm. Between the 1–2 m depth, we found an increase of 40% (+203 Pg C) relative to the top 1 m. This means that current global estimates that only consider the first 30 cm of soil are not accounting for a massive amount of C in deeper soils, which is particularly important in peatlands and permafrost regions that are prevalent in Canada (Tarnocai et al., 2009; Hugelius et al., 2014; Loisel et al., 2014). Almost half of the country is covered by permafrost, in which frozen conditions prevent C from being released into the atmosphere. Further, peatlands cover approximately 12% of Canada (Tarnocai et al., 2011) and their predominantly wet conditions greatly reduce C decomposition rates (Freeman et al., 2001),which explains the high SOC stock in these areas. The Group Global Peatland Database (Joosten, 2009) suggests that the entire area of global peatlands (3.8 million $km^2$) stores 447 Pg C in their total depth, an estimate considered conservative according to Köchy et al. (2015) because of incomplete data coverage in many regions. Later, Jackson et al. (2017) reported a total of 543 Pg C stored in global peatlands, while Hugelius et al. (2020) reported 415 ± 150 Pg C only in northern peatlands, which they estimated to have an extension of 3.7 million $km^2$ and an average of ~2.5 m depth. According to our estimates, Canadian peatlands store 142 Pg C in the top 2-meter depth, which is in line with values reported by Tarnocai (2006), who estimated 147 Pg C for the total peat depth. Our results showed that C stored in Canadian peatlands account for 34% of the amount described by Hugelius et al. (2020) and more than the SOC stock estimated for all tropical peatlands, i.e. ~110 Pg C (Page et al., 2011; Dargie et al., 2017).

The results of this study support the recent findings of Beaulne et al. (2021), who reported that peat layers, with an average between 22.6–66.0 kg $m^{-2}$, store much more C than AGB and BGB of boreal forests in Canada (2.8-5.7 kg $m^{-2}$). Our results are particularly striking for the Hudson Plain ecozone, where SOC stocks are ~150 kg C $m^{-2}$ for the top 2-meter depth. When studying C fluxes in an eco-district of Hudson Plain, McLaughlin et al. (2018) reported an average of 101 kg C $m^{-2}$ and emphasized vulnerabilities of this C pool with increasing temperatures. In fact, our study shows that the greatest amount of SOC stock is found in the Hudson Plain, a region predominantly composed of peatlands. For this ecozone, we report 52 Pg C in the top 2-meter depth, 22 Pg C more than that previously reported by Packalen et al. (2014), although those estimates were developed using a set of peat core sampling points and were not tied to a specific depth. Nevertheless, our study found large uncertainties when mapping the SOC stock in the Hudson Plain ecozone, which we can attribute to scarcity of ground training data, in addition to uncertainties in peatland depth and coarse fragment information. In addition to the Hudson Plain, forested ecozones, such as Boreal Shield and Pacific Maritime, also show higher SOC stock values (Fig. S4) which can be explained not only by the presence of peatlands and wetlands in general (Tarnocai et al., 2011; Lacourse et al., 2019) but also by the larger biomass production in forested peatlands and associated high C densities of woody peat.

Considering the potential C stock in deep soils of Canada, we also estimated SOC stock between 2–4 m depths, and we observed an increase of about +1,000 Pg C. However, due the fewer samples and the lack of information of rooting depth and coarse fragment in deeper soils, we opted to exclude this depth interval from further analysis. Still, few studies estimated SOC stock in deeper soils and most have reported high SOC stock values. Jobbagy and Jackson (2000) reported 56% more C between 1–3 m than in the top 1 m in a global scale. Batjes (2016) reported a global SOC stock of 1,408 Pg C for the top meter and 2,060 Pg C at 0-2 m depth, highlighting the large C stocks located in the Northern Circumpolar region (411 ± 65 Pg C in 0-1 m) that involves 40% of Canada's territory. In this region, Tarnocai et al. (2009) estimated 1,024 Pg C between 0-3 m depth, while the first 30 cm only account for ~18% of this value. According to Hossain et al. (2007), the SOC stock in deeper soils is high in northern regions because of strong alternate freeze-thaw actions.

## 4.2 Implication of Canada's national carbon stock mapping

In this study, we quantified and mapped the C stock size and distribution in terrestrial ecosystems of Canada using a machine learning approach and several covariates mainly composed by long-term satellite data. Unlike previous estimates, we quantified C stock of all plant components, and it was the first time that canopy height information derived from satellite LiDAR was included as covariates to estimate AGB for Canada. We also provided the first national map of SOC stock, including estimates in deep soils and peatlands, and uncertainty maps for both C stocks in forest AGB and soil.

The results indicated that Canada contains even more SOC than what was reported in global estimates, ranging from 313 Pg C in the top 1 m, to 516 Pg C in the top 2 m depth. This confirms that SOC stock estimates that are limited to the top 30 cm and exclude peatlands seriously underestimate C stocks. Our study confirms the very large SOC pool in the Hudson Plain ecozone, and also shows very large SOC pools in deep soils in the Boreal Shield region between the provinces of Ontario and Manitoba. This region is characterized by forested peatlands and studies in Quebec confirm the importance these ecosystems have to SOC stocks (Beaulne et al., 2021), yet they remain under-sampled in terms of peat depths and soil carbon densities.

This study fills some major gaps and uncertainties in the C stock estimation in terrestrial ecosystems of Canada. The estimated size and spatial distribution of the total C stocks in Canada suggest the important role of the country in the global organic C storage. This knowledge is a key step to plan and implement the stored C stock vulnerability assessment and climate change mitigation strategies. This is particularly relevant for boreal forests, where the rate of C accumulation is decreasing by fire and harvest (Wang et al., 2021), and for peatlands, where the fate of the stored large soil C stock under projected climate change, soil and permafrost thaw, fire and disturbance regimes is unknown. Peat fires are becoming increasingly common in Canada (Thompson et al., 2019). In future studies, the maps provided by this study can be used to understand the vulnerability of C stocks to human actions or climate change, such as C removal by decomposition, fires, harvesting, and other disturbances. They can also be employed as input in ecosystem or Earth system models to assess the sensitivity and feedback of C stock to future climate change, for instance, in models already being used to quantify C emissions in Canada, such as the Carbon Budget Model of the Canadian Forest Sector (CBM-CFS3) (Kurz et al., 2009), the Canadian Land Surface Scheme Including biogeochemical Cycles (CLASSIC) (Melton et al., 2020), and the Canadian model for peatlands (CaMP) (Bona et al., 2020). Because of the large magnitude and uncertainties found in the estimated C stock in peat soils, future studies should collect more ground samples in these areas to build a new C stock map specifically for Canadian peatlands, in addition to allowing for independent validation of the current map.

## Acknowledgments, Samples, and Data

This work was supported by World Wildlife Fund Canada (WWF-Canada). A.G. acknowledges funding from Natural Sciences and Engineering Research Council of Canada Discovery Grant (RGPIN-2020-05708) and the Canada Research Chairs Program.

Samples and data used and generated in this study can be found in the following sources:

- AGB samples (nfi.nfis.org) and (catalogue.data.gov.bc.ca)
- Soil samples (https://www.isric.org/) and (https://peatlands.lehigh.edu/)
- USGS Landsat 8 Surface Reflectance (https://developers.google.com/earth-engine/datasets/catalog/LANDSAT_LC08_C01_T1_SR)
- ESA Sentinel 2 Surface Reflectance (https://developers.google.com/earth-engine/datasets/catalog/COPERNICUS_S2_SR)
- Landsat 8 Collection 1 Tier 1 32-Day NDWI Composite (https://developers.google.com/earth-engine/datasets/catalog/LANDSAT_LC08_C01_T1_32DAY_NDWI)
- MODIS Terra Vegetation Indices 16-Day Global 250m (NDVI and EVI) (https://developers.google.com/earth-engine/datasets/catalog/MODIS_006_MOD13Q1)
- MCD43A3.006 MODIS White Sky Albedo (WSA) Daily 500m (https://developers.google.com/earth-engine/datasets/catalog/MODIS_006_MCD43A3)
- MODIS Global Terrestrial Evapotranspiration 8-Day Global 1km (https://developers.google.com/earth-engine/datasets/catalog/MODIS_NTSG_MOD16A2_105)
- MODIS Terra Land Surface Temperature and Emissivity Daily Global 1km (https://developers.google.com/earth-engine/datasets/catalog/MODIS_006_MOD11A1)
- MODIS Long-term Land Surface Temperature daytime monthly standard deviation (https://doi.org/10.5281/zenodo.1420114)
- ALOS DSM: Global 30m (https://developers.google.com/earth-engine/datasets/catalog/JAXA_ALOS_AW3D30_V3_2)
- Global ALOS PALSAR-2/PALSAR Yearly Mosaic (https://developers.google.com/earth-engine/datasets/catalog/JAXA_ALOS_PALSAR_YEARLY_SAR)
- Global Foliage Clumping Index data derived from MODIS BRDF (https://daac.ornl.gov/VEGETATION/guides/Global_Clumping_Index.html)
- Sentinel-1 SAR GRD (https://developers.google.com/earth-engine/datasets/catalog/COPERNICUS_S1_GRD)
- Soil types (https://sis.agr.gc.ca/cansis/nsdb/slc/index.html)
- Daymet data (https://developers.google.com/earth-engine/datasets/catalog/NASA_ORNL_DAYMET_V4)

- Spatial distribution of maximum canopy height and heights percentiles (https://doi.org/10.4121/14573079.v1)
- Forest carbon stock and uncertainty maps (https://doi.org/10.4121/14572929.v1)
- Soil carbon stock and uncertainty maps (https://doi.org/10.4121/14573526.v1)

## References


Baig, M. H. A., Zhang, L., Shuai, T., & Tong, Q. (2014), Derivation of a tasseled cap transformation based on Landsat 8 at-satellite reflectance. *Remote Sensing Letters, 5*(5), 423-431. https://doi.org/10.1080/2150704X.2014.915434

Bar-On, Y. M., Phillips, R., & Milo, R. (2018) The biomass distribution on Earth. Proc Natl Acad Sci USA, 115(25), 6506–6511. https://doi.org/10.1073/pnas.1711842115

Batjes, N. H. (2016), Harmonized soil property values for broad-scale modelling (WISE30sec) with estimates of global soil carbon stocks. *Geoderma, 269*, 61 – 68. https://doi.org/10.1016/j.geoderma.2016.01.034

Batjes, N. H., Ribeiro, E., van Oostrum, A., Leenaars, J., Hengl, T., & Mendes de Jesus, J. (2017), WoSIS: providing standardised soil profile data for the world. *Earth Syst. Sci. Data, 9*, 1–14.

Beaudoin, A., Bernier, P.Y., Guindon, L., Villemaire, P., Guo, X. J., Stinson, G., et al. (2014), Mapping attributes of Canada's forests at moderate resolution through k NN and MODIS imagery. *Can. J. For. Res., 44*, 521–532. https://doi.org/10.1139/cjfr-2013-0401

Beaulne, J., Garneau, M., Magnan, G., & Boucher, E. (2021), Peat deposits store more carbon than trees in forested peatlands of the boreal biome. *Sci. Rep.*, *11*, 2657. 10.1038/s41598-021-82004-x

Bona, K. N., Shaw, C., Thompson, D. K., Hararuk, O., Webster, K., Zhang, G., Voicu, M., & Kurz, W. A. (2020), The Canadian model for peatlands (CaMP): A peatland carbon model for national greenhouse gas reporting. *Ecol. Model.*, *431*, 109164. https://doi.org/10.1016/j.ecolmodel.2020.109164

Breiman, L. (2001), Random Forests. *Machine Learning, 45*(1), 5–32. https://doi.org/10.1023/A:1010933404324

Bush, E., & Flato, G. (2019), About this report; Chapter 1 in *Canada's Changing Climate Report*, (ed.) E. Bush and D.S. Lemmen; Government of Canada, Ottawa, Ontario, p. 7–23.

Christensen, T. (1991), Arctic and sub-Arctic soil emissions: Possible implications for global climate change. *Polar Record, 27*, 205–210. https://doi.org/10.1017/S0032247400012584

Dargie, G. C., Lewis, S. L., Lawson, I. T., Mitchard, E. T. A., Page, S. E., Bocko, Y. E., & Ifo, S. A. (2017), Age, extent and carbon storage of the central Congo Basin peatland complex. *Nature, 542*, 86–90. https://doi.org/10.1038/nature21048

Daughtry, C. S. T., Walthall, C. L., Kim, M. S., Brown de Colstoun, E., & McMurtrey, J. E. (2000), Estimating corn leaf chlorophyll concentration from leaf and canopy reflectance. *Remote Sens. Environ., 74*(2), 229–239. https://doi.org/10.1016/S0034-4257(00)00113-9

Davidson, E. A., & Janssens, I. A. (2006), Temperature sensitivity of soil carbon decomposition and feedbacks to climate change. *Nature, 440*, 165–173. https://doi.org/10.1038/nature04514

Deng, A., & Stauffer, D. R. (2006), On improving 4-km mesoscale model simulations. *Journal of Applied Meteorology and Climatology*, *45*(3), 361–381. doi:10.1175/JAM2341.1

Didan. K. (2015), MOD13Q1 MODIS/Terra Vegetation Indices 16-Day L3 Global 250m SIN Grid V006, distributed by NASA EOSDIS Land Processes DAAC.

Duncanson, L., Neuenschwander, A., Hancock, S., Thomas, N., Fatoyinbo, T., Simard, M., et al. (2020), Biomass estimation from simulated GEDI, ICESat-2 and NISAR across environmental gradients in Sonoma County, California. *Remote Sens. Environ., 242*, 111779. https://doi.org/10.1016/j.rse.2020.111779

European Space Agency. Sentinel-1: Overview. Available at: https://sentinel.esa.int/web/sentinel/missions/sentinel-1/overview

European Space Agency. Sentinel-2 MSI: Overview. Available at: <https://sentinel.esa.int/web/sentinel/user-guides/sentinel-2-msi/overview>

FAO (2018), Global Soil Organic Carbon Map (GSOCmap) Technical Report. Rome. 162 pp.

FAO (2020a), Global Forest Resources Assessment 2020: *Main report*. Rome, 164pp.

FAO (2020b), Global Forest Resources Assessment 2020: *Canada*. Rome, 70pp.

FAO, IIASA, ISRIC, ISS-CAS, & JRC (2012), Harmonized World Soil Database (version 1.2). FAO, Rome, Italy and IIASA, Laxenburg, Austria.

Frampton, W. J.; Dash, J., Watmough, G., & Milton, E. J. (2013), Evaluating the capabilities of Sentinel-2 for quantitative estimation of biophysical variables in vegetation. *ISPRS J. Photogramm. Remote Sens., 82*, 83–92. https://doi.org/10.1016/j.isprsjprs.2013.04.007

Freeman, C., Ostle, N., & Kang, H. (2001), An enzymic 'latch' on a global carbon store. *Nature, 409*(149). https://doi.org/10.1038/35051650

Gallego-Sala, A. V., Charman, D. J., Brewer, S., Page, S. E., Prentice, I. C., Friedlingstein, P., Moreton, S., & Amesbury, M. J. (2018), Latitudinal limits to the predicted increase of the peatland carbon sink with warming. *Nat. Clim. Chang., 8*, 907-913. https://doi.org/10.1038/s41558-018-0271-1

Gao, B. (1996), NDWI—A normalized difference water index for remote sensing of vegetation liquid water from space. *Remote Sens. Environ., 58*(3), 257-266. https://doi.org/10.1016/S0034-4257(96)00067-3

Goetz, S., & Dubayah, R. (2011), Advances in remote sensing technology and implications for measuring and monitoring forest carbon stocks and change. *Carbon Management, 2*, 231-244. https://doi.org/10.4155/cmt.11.18

Gonsamo, A., Chen, J. M., Colombo, S. J., Ter-Mikaelian, M. T., & Chen, J. (2017), Global change induced biomass growth offsets carbon released via increased forest fire and respiration of the central Canadian boreal forest. *J. Geophys. Res. Biogeosci., 122*, 1275-1293. https://doi.org/10.1002/2016JG003627

Gonsamo, A., Chen, J. M., Price, D. T., Kurz, W. A., Liu, J., Boisvenue, C., Hember, R. A., Wu, C., & Chang, K. H. (2013), Improved assessment of gross and net primary productivity of

Canada's landmass. *J. Geophys. Res. Biogeosci., 118*, 1546–1560. https://doi.org/10.1002/2013JG002388

Government of Canada (2019), 2015 Land Cover of Canada. Available at: https://open.canada.ca/data/en/dataset/4e615eae-b90c-420b-adee-2ca35896caf6.

Haboudane, D., Miller, J. R., Tremblay, N., Zarco-Tejada, P. J., & Dextraze, L. (2002), Integrated narrow-band vegetation indices for prediction of crop chlorophyll content for application to precision agriculture. *Remote Sens. Environ., 81*(2-3), 416–426. https://doi.org/10.1016/S0034-4257(02)00018-4

Harris, N. L., Gibbs, D. A., Baccini, A., Birdsey, R. A., Bruin, S. de, Farina, M., et al. (2021), Global maps of twenty-first century forest carbon fluxes. *Nat. Clim. Chang., 11*, 234–240. https://doi.org/10.1038/s41558-020-00976-6

He, L., Chen, J. M., Pisek, J., Schaaf, C., & Strahler, A. (2017), Global 500-m Foliage Clumping Index Data Derived from MODIS BRDF, 2006. ORNL DAAC, Oak Ridge, Tennessee, USA.

Heimann, M. & Reichstein, M. (2008), Terrestrial ecosystem carbon dynamics and climate feedbacks. *Nature, 451*, 289–292. https://doi.org/10.1038/nature06591

Hengeveld, H. G. (2000), Projections for Canada’s climate future: A discussion of recent simulations with the Canadian Global Climate Model. Climate Change Digest, CCD 00-01, Special Edition. Downsview, Ontario: Meteorological Service of Canada, Environment Canada.

Hengl, T. (2018), Long-term MODIS LST day-time and night-time temperatures, sd and differences at 1 km based on the 2000–2017 time series.

Hengl, T., & MacMillan, R. A. (2019), *Predictive Soil Mapping with R*. Wageningen, Netherlands: Open Geo Hub foundation, 370pp.

Hengl, T., Mendes de Jesus, J., MacMillan, R. A., Batjes, N. H., Heuvelink, G. B. M., Ribeiro, E., et al. (2014), SoilGrids1km —Global Soil Information Based on Automated Mapping. *PLoS ONE, 9*, e105992. https://doi.org/10.1371/journal.pone.0105992

Hengl, T., Mendes, J., Heuvelink, G. B. M., Gonzalez, M. R., Kilibarda, M., Blagotić, A., et al. (2017), SoilGrids250m: Global gridded soil information based on Machine Learning. *PLoS ONE*, *12*(2), e0169748. https://doi.org/10.1371/journal.pone.0169748

Hossain, M. F., Chen, W., & Zhang, Y. (2015), Bulk Density of Mineral and Organic Soils in the Canada’s Arctic and Sub-Arctic. *Information Processing in Agriculture, 2*(3), 183-190. https://doi.org/10.1016/j.inpa.2015.09.001

Hossain, M. F., Zhang, Y., Chen, W., Wang, J., & Pavlic, G. (2007), Soil organic carbon content in northern Canada: A database of field measurements and its analysis. *Can. J. Soil Sci., 87*, 259–268. https://doi.org/10.4141/S06-029

Hugelius, G., Loisel, J., Chadburn, S., Jackson, R. B., Jones, M., MacDonald, G., et al. (2020), Large stocks of peatland carbon and nitrogen are vulnerable to permafrost thaw. *Proc. Natl. Acad. Sci. U S A, 117*(34), 20438-20446. https://doi.org/10.1073/pnas.1916387117

Hugelius, G., Strauss, J., Zubrzycki, S., Harden, J. W., Schuur, E. A. G., Ping, C. L., et al. (2014), Estimated stocks of circumpolar permafrost carbon with quantified uncertainty ranges and identified data gaps. *Biogeosci., 11*(23), 6573-6593. https://doi.org/10.5194/bg-11-6573-2014

IPCC - Intergovernmental Panel on Climate Change (2006), IPCC Guidelines for National Greenhouse Gas Inventories; Prepared by the National Greenhouse Gas Inventories Programme; Eggleston, H. S., Buendia, L., Miwa, K., Ngara, T., & Tanabe, K., Eds.; Japan Institute for Global Environmental Strategies: Hayama, Japan (2006).

IPCC, Summary for Policymakers and Technical Summary (2007). In: *Climate Change 2007: The Physical Science Basis*. Contribution of Working Group I to the Fourth Assessment Report of the Intergovernmental Panel on Climate Change [S. Solomon, D. Qin, M. Manning, Z. Chen, M. Marquis, K.B. Averyt, M. Tignor, H.L. Miller (eds.)]. Cambridge University Press, Cambridge, United Kingdom and New York, NY, USA (2007).

Jackson, R. B., Lajtha, K., Crow, S. E., Hugelius, G., Kramer, M. G., & Piñeiro, G. (2017), The Ecology of Soil Carbon: Pools, Vulnerabilities, and Biotic and Abiotic Controls. *Annual Review of Ecology, Evolution, and Systematics, 48*(1), 419-445. https://doi.org/10.1146/annurev-ecolsys-112414-054234

Jobbagy, E. G., & Jackson, R. B. (2000), The vertical distribution of soil organic carbon and its relation to climate and vegetation. *Ecol. Appl., 10*, 423–436. https://doi.org/10.1890/1051-0761(2000)010[0423:TVDOSO]2.0.CO;2

Joosten, H. (2009), The global peatland CO2 picture. Peatland status and emissions in all countries of the world. *Environmental Science*.

Jordan, C. F. (1969), Derivation of leaf-area index from quality of light on the forest floor. *Ecology, 50*(4), 663–666. https://doi.org/10.2307/1936256

Köchy, M., Hiederer, R., & Freibauer, A. (2015), Global distribution of soil organic carbon—Part 1: Masses and frequency distributions of SOC stocks for the tropics, permafrost regions, wetlands, and the world. *The Soil, 1*, 351–365. https://doi.org/10.5194/soil-1-351-2015.

Kumar, L., & Mutanga, O. (2017), Remote Sensing of Above-Ground Biomass. *Remote Sens., 9*(9), 935. https://doi.org/10.3390/rs9090935

Kurz, W. A., & Apps, M. J. (1999), 70-year retrospective analysis of carbon fluxes in the Canadian forest sector. *Ecol. Appl., 9*(2), 526–547.

Kurz, W. A., Dymond, C. C., White, T. M., Stinson, G., Shaw, C. H., Rampley, G. J., et al. (2009), CBM-CFS3: A model of carbon-dynamics in forestry and land-use change implementing IPCC standards. *Ecol. Model., 220*(4). https://doi.org/10.1016/j.ecolmodel.2008.10.018

Lacourse, T., Adeleye, M. A., & Stewart, J. R. (2019). Peatland formation, succession and carbon accumulation at a mid-elevation poor fen in Pacific Canada. *The Holocene, 29*(11), 1694-1707. https://doi.org/10.1177/0959683619862041

Li, Z., Kurz, W. A., Apps, M. J., & Beukema, S. J. (2003), Belowground biomass dynamics in the Carbon Budget Model of the Canadian Forest Sector: recent improvements and implications for the estimation of NPP and NEP. *Can. J. For. Res., 33*(1), 126–136. https://doi.org/10.1139/x02-165

Loisel, J., Gallego-Sala, A.V., Amesbury, M. J., Magnan, G., Anshari, G., Beilman, D. W., et al. (2021), Expert assessment of future vulnerability of the global peatland carbon sink. *Nat. Clim. Chang., 11*, 70–77. https://doi.org/10.1038/s41558-020-00944-0

Loisel, J., Yu, Z., Beilman, D. W., Camill, P., Alm, J., Amesbury, M. J., et al. (2014), A database and synthesis of northern peatland soil properties and Holocene carbon and nitrogen accumulation. *The Holocene, 24*(9), 1028–1042. https://doi.org/10.1177/0959683614538073

Mahdianpari, M., Brisco, B., Granger, J. E., Mohammadimanesh, F., Salehi, B., Banks, S., et al. (2020), The Second Generation Canadian Wetland Inventory Map at 10 Meters Resolution Using Google Earth Engine. *Can. J. Remote Sens., 46*, 3, 360-375. https://doi.org/10.1080/07038992.2020.1802584

Matasci, G., Hermosilla, T., Wulder, M. A., White, J. C., Coops, N. C., Hobart, G. W., & Zald, H. S. (2018a), Large-area mapping of Canadian boreal forest cover, height, biomass and other structural attributes using Landsat composites and lidar plots. *Remote Sens. Environ., 209*, 90–106. https://doi.org/10.1016/j.rse.2017.12.020

Matasci, G., Hermosilla, T., Wulder, M. A., White, J. C., Coops, N. C., Hobart, G. W., et al. (2018b), Three decades of forest structural dynamics over Canada's forested ecosystems using Landsat time-series and lidar plots. *Remote Sens. Environ., 216*, 697-714. https://doi.org/10.1016/j.rse.2018.07.024

McLaughlin, J., Packalen, M., & Shrestha, B. (2018), Assessment of the vulnerability of peatland carbon in the Albany Ecodistrict of the Hudson Bay Lowlands, Ontario, Canada to climate change. *Climate Change Research Report* CCRR-46, 40 pp., Ontario Ministry of Natural Resources and Forestry Science and Research Branch, Peterborough, ON, Canada.

Meinshausen, N. (2006), Quantile Regression Forests. *Journal of Machine Learning Research, 7*, 983–999.

Melton, J. R., Arora, V. K., Wisernig-Cojoc, E., Seiler, C., Fortier, M., Chan, E., & Teckentrup, L. (2020), CLASSIC v1.0: the open-source community successor to the Canadian Land Surface Scheme (CLASS) and the Canadian Terrestrial Ecosystem Model (CTEM) – Part 1: Model framework and site-level performance. *Geosci. Model Dev., 13*, 2825–2850. https://doi.org/10.5194/gmd-13-2825-2020

Merzlyak, M. N., Gitelson, A. A., Chivkunova, O. B., & Rakitin, V. Y. (1999), Non-destructive optical detection of pigment changes during leaf senescence and fruit ripening. *Physiol. Plant., 106*(1), 135–141. https://doi.org/10.1034/j.1399-3054.1999.106119.x

Minasny, B., Berglund, Ö., Connolly, J., Hedley, C., deVries, F., Gimona, A. et al. (2019), Digital mapping of peatlands – a critical review. *Earth Sci. Rev., 196*. https://doi.org/10.1016/j.earscirev.2019.05.014

Mu, Q., Zhao, M., Running, & S. W. (2014), Numerical Terradynamic Simulation Group. MODIS Global Terrestrial Evapotranspiration (ET) Product MOD16A2 Collection 5.

Narine, L., Popescu, S. C., & Malambo, L. (2019), Synergy of ICESat-2 and Landsat for Mapping Forest Aboveground Biomass with Deep Learning. *Remote Sens., 11*, 1503. https://doi.org/10.3390/rs11121503

National Forest Inventory (NFI) (2016), Canada National Forest Inventory Customized Report. Available at: https://nfi.nfis.org/en/customized_report.

Nelson, D. W., & Sommers, L. (1982), Total carbon, organic carbon, and organic matter. In: Page, A., Miller, R., Keeney, D., editors, *Methods of soil analysis*, Part 2, Madison, WI: ASA and SSSA, Agron. Monogr., 9. 2nd edition, 539–579.

Neuenschwander, A. & Pitts, K. (2019), The ATL08 land and vegetation product for the ICESat-2 mission. *Remote Sens. Environ., 221*, 247-259. https://doi.org/10.1016/j.rse.2018.11.005

NSDB - National Soil Database. Soil Landscape of Canada version 3.2. 2011. http://sis.agr.gc.ca/cansis/nsdb/slc/index.html.

Packalen, M., Finkelstein, S. A., & McLaughlin, J. (2014), Carbon storage and potential methane production in the Hudson Bay Lowlands since mid-Holocene peat initiation. *Nat. Commun., 5*, 4078. https://doi.org/10.1038/ncomms5078

Page, S. E., Rieley, J. O., & Banks, C. J. (2011), Global and regional importance of the tropical peatland carbon pool. *Glob. Change Biol., 17*(2), 798–818. https://doi.org/10.1111/j.1365-2486.2010.02279.x

Pennock, D. J., Watson, K., & Sanborn, P. (2015), Section 4. Horizon identification. From: Pennock, D. J., Watson, K., Sanborn, P. Field Handbook for the Soils of Western Canada. Canadian Society of Soil Service.

Qi, W., Saarela, S., Armston, J., Stahl, G., & Dubayah, R. (2019), Forest biomass estimation over three distinct forest types using TanDEM-X InSAR data and simulated GEDI lidar data. *Remote Sens. Environ., 232*, 111283. https://doi.org/10.1016/j.rse.2019.111283

Ribeiro, E., Batjes, N. H, Leenaars, J. G. B., & van Oostrum, A. (2015), Towards the standardization and harmonization of world soil data. *ISRIC Report 2015/03*. Wageningen, the Netherlands: ISRIC—World Soil Information.

Richardson, A. J., & Weigand, C. (1977), Distinguishing vegetation from soil background information. *Photogramm. Eng. Remote Sensing, 43*(12), 1541-1552.

Riggs, G. A., Hall, D. K., & Salomonson, V. V. (1994), A snow index for the Landsat Thematic Mapper and Moderate Resolution Imaging Spectroradiometer, paper presented at the IEEE International Geoscience and Remote Sensing Symposium, Pasadena, CA, USA, 1994, 1942-1944 v. 4.

Riley, S. J., de Gloria, S. D., & Elliot, R. A. (1999), Terrain Ruggedness that Quantifies Topographic Heterogeneity. *Intermountain Journal of Science*, *5*(1-4), 23-27.

Rodríguez-Veiga, P., Wheeler, J., Louis, V., Tansey, K., & Balzter, H. (2017), Quantifying Forest Biomass Carbon Stocks From Space. *Curr. Forestry Rep., 3,* 1–18. https://doi.org/10.1007/s40725-017-0052-5.

Rondeaux, G., Steven, M., & Baret, F. (1996), Optimization of soil-adjusted vegetation indices. Remote Sens. Environ., 55(2), 95–107. https://doi.org/10.1016/0034-4257(95)00186-7

Sanderman, J., Hengl, T., Fiske, G., Solvik, K., Adame, M. F., Benson, L., et al. (2018), A global map of mangrove forest soil carbon at 30m spatial resolution. *Environ. Res. Lett., 13*, 055002.

Schaaf, C., & Wang, Z. (2015), MCD43A3 MODIS/Terra+Aqua BRDF/Albedo Daily L3 Global - 500m V006. (2015), distributed by NASA EOSDIS Land Processes DAAC.

Scharlemann, J. P., Tanner, E. V., Hiederer, R., & Kapos, V. (2014), Global soil carbon: Understanding and managing the largest terrestrial carbon pool. *Carbon Management, 5*(1), 81–91. https://doi.org/10.4155/cmt.13.77

Shimada, M., Itoh, T., Motooka, T., Watanabe, M., Tomohiro, S., Thapa, R., & Lucas, R. (2014), New Global Forest/Non-forest Maps from ALOS PALSAR Data (2007-2010). Remote Sens. Environ., 155, 13-31. https://doi.org/10.1016/j.rse.2014.04.014

Spawn, S. A., Sullivan, C. C., Lark, T. J., & Gibbs, H. K. (2020), Harmonized global maps of above and belowground biomass carbon density in the year 2010. *Sci Data, 7*(112). https://doi.org/10.1038/s41597-020-0444-4

Takaku, J., Tadono, T., Tsutsui, K., & Ichikawa, M. (2016), Validation of 'AW3D' Global DSM Generated from ALOS PRISM, ISPRS Annals of the Photogrammetry, Remote Sensing and Spatial Information Sciences III-4, 25-31.

Tarnocai, C. (2006), The effect of climate change on carbon in Canadian peatlands. *Global and Planetary Change, 53*(4) 222–232. https://doi.org/10.1016/j.gloplacha.2006.03.012

Tarnocai, C. (2009), The Impact of Climate Change on Canadian Peatlands. *Canadian Water Resources Journal*, *34*(4), 453–466. https://doi.org/10.4296/cwrj3404453

Tarnocai, C., Canadell, J. G., Schuur, E. A. G., Kuhry, P., Mazhitova, G., & Zimov, S. (2009), Soil organic carbon pools in the northern circumpolar permafrost region. *Global Biogeochem. Cy., 23*, GB2023. https://doi.org/10.1029/2008GB003327

Tarnocai, C., Kettles, I. M., & Lacelle, B. (2011), Peatlands of Canada. *Geological Survey of Canada*, Open File 6561.

Thompson, D. K., Simpson, B. N., Whitman, E., Barber, Q. E., & Parisien, M.-A. (2019), Peatland Hydrological Dynamics as A Driver of Landscape Connectivity and Fire Activity in the Boreal Plain of Canada. *Forests, 10*(7), 534. https://doi.org/10.3390/f10070534

Thornton, P. E., Thornton, M. M., Mayer, B. W., Wilhelmi, N., Wei, Y., Devarakonda, R., & Cook, R. B. (2014), Daymet: Daily Surface Weather Data on a 1-km Grid for North America, Version 2. ORNL DAAC, Oak Ridge, Tennessee, USA.

Tifafi, M., Guenet, B., & Hatté, C. (2017), Large differences in global and regional total soil carbon stock estimates based on SoilGrids, HWSD, and NCSCD: Intercomparison and Evaluation Based on Field Data From USA, England, Wales, and France. *Global Biogeochem. Cy., 32*, 42 –56. https://doi.org/10.1002/2017GB005678

Turetsky, M., Benscoter, B., Page, S., Rein, G., van der Werf, G. R., & Watts, A. (2015), Global vulnerability of peatlands to fire and carbon loss. *Nature Geosci., 8*, 11–14. https://doi.org/10.1038/ngeo2325

U.S. Geological Survey, 2015, Landsat surface reflectance data (ver. 1.1, March 27, 2019): U.S. Geological Survey Fact Sheet 2015-3034, 1 p.

Wan, Z., Hook, S., & Hulley, G. (2015), MOD11A1 MODIS/Terra Land Surface Temperature/Emissivity Daily L3 Global 1km SIN Grid V006, distributed by NASA EOSDIS Land Processes DAAC.

Wang, J. A., Baccini, A., Farina, M.  Randerson, J. T., & Friedl, M. A. (2021), Disturbance suppresses the aboveground carbon sink in North American boreal forests. Nat. Clim. Chang. https://doi.org/10.1038/s41558-021-01027-4

Webster, K. L., Bhatti, J. S., Thompson, D. K., Nelson, S. A., Shaw, C. H., Bona, K. A., et al. (2018), Spatially-integrated estimates of net ecosystem exchange and methane fluxes from Canadian peatlands. *Carbon Balance Manage*, *13*(16). https://doi.org/10.1186/s13021-018-0105-5

Wilson, J. P., & Gallant, J. C. (2000), Terrain Analysis - Principles and Applications. 520pp.

Wu, C., Niu, Z., Tang, Q., & Huang, W. (2008), Estimating chlorophyll content from hyperspectral vegetation indices: modeling and validation. *Agric. For. Meteorol.*, *148*(8-9), 1230–1241. https://doi.org/10.1016/j.agrformet.2008.03.005

Wulder, M. A., Hermosilla, T., White, J. C., & Coops, N. C. (2020), Biomass status and dynamics over Canada's forests: Disentangling disturbed area from associated aboveground biomass consequences. *Environ. Res. Lett.*, *15*(9), 094093. https://doi.org/ 10.1088/1748-9326/ab8b11

Xu, J., Morris, P. J., Liu, J., & Holden, J. (2018), PEATMAP: Refining estimates of global peatland distribution based on a meta-analysis. *CATENA*, *160*, 134-140. https://doi.org/10.1016/j.catena.2017.09.010

Yu, Z. C. (2012), Northern peatland carbons stocks and dynamics: a review. *Biogeosci.*, *9*, 4071–4085. https://doi.org/10.5194/bg-9-4071-2012

Zhang, X., Chen, X., Tian, M., Fan, Y., Ma, J., & Xing, D. (2020), An evaluation model for aboveground biomass based on hyperspectral data from field and TM8 in Khorchin grassland, China. *PLoS ONE*, *15*(2), e0223934. https://doi.org/10.1371/journal.pone.0223934